This article has been accepted for inclusion in a future issue of this journal. Content is final as presented, with the exception of pagination.

Operation of a Gyromagnetic Line at Low and High Voltages With Simultaneous Axial and Azimuthal Biases

Fernanda S. Yamasaki, *Member, IEEE*, Jose O. Rossi, *Senior Member, IEEE*, Joaquim J. Barroso, *Member, IEEE*, and Edl Schamiloglu, *Fellow, IEEE*

***Abstract*— A great interest has been devoted to the study of nonlinear transmission lines (NLTLs) for radio frequency (RF) generation since they have been used with great success in RF generation by producing a train of oscillatory waves along the line and at its output. There are two configurations of NLTLs. The first one is a dispersive line consisting of *LC* sections with nonlinear components, and the second one is a continuous ferrite loaded nondispersive line generally biased by an axial magnetic field, known as gyromagnetic line. In this paper, the focus of the study is on the second one, since gyromagnetic lines can operate in a broader frequency range (0.3–2.0 GHz) with higher conversion efficiency (20.0%) when compared to lumped NLTLs, generally limited up to 300 MHz with less than 10.0% of efficiency, because of their dielectric losses and stray impedances on line structure. Different models have been used along the years by several authors with different approaches to study the gyromagnetic phenomenon by means of numerical simulations based on analytical models to predict the precession movement of the electron magnetic dipole of the ferromagnetic material. Thus, the goal of this paper is to analyze the gyromagnetic NLTL behavior through the effects on the line operation. The novelty herein is to use two biases simultaneously to study continuous gyromagnetic NLTLs, focusing on the pulse rise time compression and RF generation caused by the precession of the magnetic dipole. An experimental setup is described and tested for low- and high-voltage operation for a 20-cm gyromagnetic line loaded with NiZn ferrite beads. The novelty of this paper is to use two biases simultaneously to study continuous gyromagnetic NLTLs, such techniques can be useful in the design of continuous lines for RF applications in space and mobile defense platforms of compact size.**

***Index Terms*— Ferrites, gyromagnetism, nonlinear transmission line (NLTL), pulse shaping circuits, radio frequency (RF) generation.**

Manuscript received June 26, 2017; revised February 8, 2018; accepted May 20, 2018. This work was supported by the Southern Office of Aerospace Research and Development (SOARD–USAF) under Grant FA9550-18-1-0111 (INPE) and Grant FA9550-15-1-0094 (UNM). The review of this paper was arranged by Senior Editor W. Jiang. *(Corresponding author: Fernanda S. Yamasaki.)*

F. S. Yamasaki and J. O. Rossi are with the Associated Plasma Laboratory, National Institute for Space Research, São José dos Campos 12227-010, Brazil (e-mail: fernandayamasaki@hotmail.com).

J. J. Barroso is with the Technological Institute of Aeronautics, São José dos Campos 12228-090, Brazil.

E. Schamiloglu is with the Electrical and Computer Engineering Department, University of New Mexico, Albuquerque, NM 87131 USA.

Color versions of one or more of the figures in this paper are available online at http://ieeexplore.ieee.org.

Digital Object Identifier 10.1109/TPS.2018.2840425

I. Introduction

THE cost of satellite launching has a direct relation with its weight (heavier, more expensive the effective cost), and consequently, emerging technologies and new materials used in satellite design enable the development of compact and more reliable materials, driving to more efficient and cheaper systems [1]. Nowadays, to establish communication between a satellite and a ground station, electronic vacuum tubes [such as traveling-wave tubes (TWTs)] are used as final amplifiers in the communication link, with excellent results so far. TWTs are used in the frequency range 300.0 MHz–50.0 GHz, with a capability of power generation from watts to megawatts and are largely used as final amplifiers in satellite communications [2]. An alternative way of reaching the same radio frequency (RF) generation produced by the TWTs to establish communication between the ground station and the satellite could be the use of nonlinear transmission lines (NLTLs) (as gyromagnetic lines) that are all solid state and of compact size not requiring thermionic cathode and vacuum. Another possible application of the gyromagnetic lines could be in pulsed radar satellites [as synthetic aperture radar (SAR)] that are used in remote sensing to provide the data and information for different applications such as climate change, deforestation detection, development of urban areas, mobility, forecast of natural disasters (hurricanes, tsunamis, volcanoes, etc.), and military area [3], [4]. The frequency range used for SAR pulse emission is in the microwave range, which occupies a large band in the frequency spectrum from 300 MHz to 300 GHz.

A great interest has been devoted to the study of NLTLs for RF generation and radiation. The two well-known configurations of NLTLs are a dispersive line, consisting of sections with nonlinear components, and a continuous nondispersive line known as a gyromagnetic line. Both configurations have the same principle of operation based on the sharpening of the input pulse, related to the dielectric permittivity variation with voltage for discrete lines and the magnetic permeability depends on current for the gyromagnetic lines.

The *LC* discrete lines and continuous nondispersive lines are conceptually different. Gyromagnetic NLTLs can produce a very broad frequency spectrum, with RF conversion efficiency of about 20% starting from 300 MHz and exceeding frequencies of 2.0 GHz [5]–[9] for potential applications in satellite

0093-3813 © 2018 IEEE. Personal use is permitted, but republication/redistribution requires IEEE permission.
See http://www.ieee.org/publications_standards/publications/rights/index.html for more information.

This article has been accepted for inclusion in a future issue of this journal. Content is final as presented, with the exception of pagination.

communications, which require operating frequencies at least in the *S*-band range. On the other hand, nonlinear discrete *LC* lines operate at lower frequencies around 1.0 GHz [10] in the case of inductive lines with saturated inductors, performing worse when relying on ceramic dielectrics, which limit their application in frequencies up to 250–300 MHz [11], [12].

The focus of this paper is on gyromagnetic lines since this line can generate stronger pulse oscillations at higher frequencies than the discrete lines, in addition to having higher RF conversion efficiency. Another advantage of the gyromagnetic lines in relation to the dispersive dielectric NLTLs is the stronger nonlinearity of the ferrite-based inductance when compared to the nonlinearity of the nonlinear ceramic capacitance or of the reverse-biased varactor diodes [13]. This paper explores and quantifies the characteristics of gyromagnetic NLTL's based on a model whereby the line is biased axially and azimuthally simultaneously for the first time, to achieve in the future a RF generation system of compact size, which will also be efficient and cheaper. This technology also presents great prospects for space and defense applications (satellites, aircraft, and so on).

A. Nonlinear Discrete LC Lines

Although the focus of this paper is on gyromagnetic lines, to have a basis comparison, the discrete lines are briefly described in this section. The discrete *LC* lines, also referred to as a nonlinear lumped element transmission line, consists of periodic sections of nonlinear inductors and/or capacitors, where a square input pulse injected onto the line will be submitted to the dispersion effect, and subsequently modulated and decomposed into a series of solitons (oscillatory pulses). This effect owes to the NLTL working principle based on a balance between two characteristic line properties: dispersion and nonlinearity. Transmission lines built with discrete elements are responsible for the dispersion effect and the elements used as varicap diodes, ceramic capacitors, and/or saturated inductors are responsible for the characteristic of nonlinearity of the line [14]–[16]. Nonlinearity and dispersion act together to provide the high-frequency oscillations along the line.

The accurate calculation of the pulse rise time reduction at the output is difficult to achieve due to the line nonlinearity and the dependence of the phase velocity on frequency in dispersive lines. However, an estimate can be made by calculating the difference between the propagation times of the portion of the pulse with lower amplitude and its peak. Therefore, for the lower portion of an input pulse propagating along a linear line, the delay is given approximately by $\delta_1 = n(LC_0)^{1/2}$, where n is the number of sections of the line. While at the peak of the propagating pulse the delay is equivalent to $\delta_2 = n(LC(V_{\max}))^{1/2}$, and therefore, according to Fig. 1, the rise time reduction of the output pulse is given in [17] $\Delta T = \delta_1 - \delta_2 = t_{\text{ri}} - t_{\text{ro}} = n((LC_0)^{1/2} - (LC(V_{\max}))^{1/2})$, where t_{ri} and t_{ro} are the input and output rise times, respectively.

B. Basic Concepts of Gyromagnetic Lines

Gyromagnetic NLTLs generate microwaves induced by the damped gyromagnetic precession of the magnetic moments in the ferromagnetic material and thus are used as compact, solid state, and RF sources [18], [19]. The output frequency of a gyromagnetic NLTL can be adjusted by controlling the bias magnetic field applied externally and by the amplitude of incident voltage pulse [20]. The output power is determined by the intrinsic properties of the ferromagnetic material and by the length of the transmission line [9].

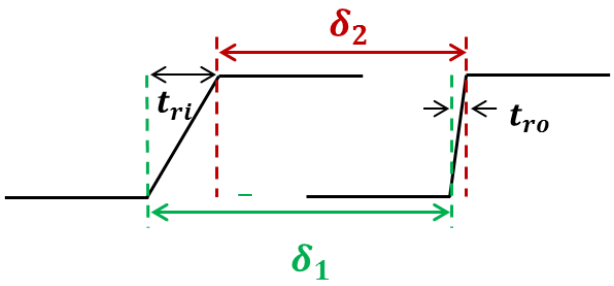

Fig. 1. Compression of the output pulse in a NLTL.

The gyromagnetic line principle of operation is based on the sharpening of the output pulse in relation to the input pulse, caused by the dependence of the magnetic permeability of the material on the current applied [21]. As the current pulse propagates down the line the magnetic permeability decreases with the current amplitude. Thus, the crest of the pulse will travel faster than its portion of lower amplitude since the propagation velocity in a nonlinear magnetic medium is given as

$$v_p = c/\sqrt{\varepsilon_r \mu_r(I)} \tag{1}$$

where c is the speed of light in vacuum, $\mu_r(I)$ is the relative magnetic permeability that varies with the current I, and ε_r is the relative electric permittivity.

As the leading edge of the input pulse with higher amplitude travels faster than the portion of smaller amplitude, the emerging output pulse becomes sharpened. As shown in Fig. 1, the pulse rise time reduction per meter along the line can be estimated as [21] $\Delta T = (LC)^{1/2} - (L_{\text{sat}}C)^{1/2}$, where L is the line inductance per meter far from saturation, L_{sat} is the saturated line inductance per meter, and finally C is the linear capacitance of the line per meter. The pulse rise time reduction is limited by the switching characteristics of the ferrite due to the time it takes to switch from one state to another on the B–H curve of the material, which is related to the relaxation frequency of the magnetic material [13].

C. Types of Bias

The coaxial line can be biased in two different ways, using azimuthal bias for pulse compression or axial bias for efficient RF generation from magnetic precession.

For pulse compression, the line is biased by a dc current flowing through the inner conductor so that the ferrites are saturated in the opposite direction to that when a current pulse is injected onto the line, also known as azimuthal bias. Indeed, pulse compression occurs even if the lines are not biased since a reset pulse is applied to degauss the line before the arrival

This article has been accepted for inclusion in a future issue of this journal. Content is final as presented, with the exception of pagination.

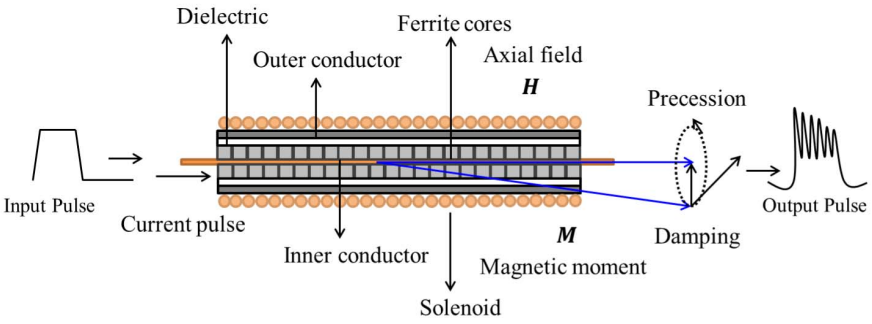

Fig. 2. Precession of the magnetic moment M in ferrites.

of the next current pulse. For RF generation, the axial bias is used where the total effective field is twisted as the azimuthal field generated by the current pulse injected onto the line is superimposed on the axial field.

Also, it is possible to improve the pulse compression with a rise time smaller than 1.0 ns by biasing the line with an axial field produced by the use of permanent magnets or a solenoid. By introducing axial bias into the line, the precession effect of the magnetic moments in the ferrite must be considered, since it causes oscillations on the amplitude of the output pulse [21]. On the other hand, for azimuthal bias, this effect is neglected.

As shown in Fig. 2, if the line is immersed in an axial magnetic field H_z, as soon as a current pulse I is injected, the magnetic moment M of the ferrite, initially aligned along the longitudinal axis, interacts with the azimuthal field generated around the conductor, leading to the pulse compression. At the same time, because of the magnetic torque, a high-frequency precession motion of the magnetic moment occurs with a dimensionless damping factor α, which depends on the characteristics of the ferrite.

The magnetic precession motion in ferrites takes place along the line as soon as the current pulse starts to propagate, inducing high-frequency oscillations on the propagating pulse. These oscillations appear superimposed on the amplitude of the output pulse with a similar shape to that of the input pulse, but with a reduced rise time. This effect can be predicted using the famous equation known today as Landau–Lifshitz–Gilbert (LLG), which was introduced first by Landau and Lifshitz in 1935 and modified later by Gilbert in 1956 [22], whose final form of the dynamics of the ferrite magnetization M is given as

$$\frac{\partial \vec{M}}{\partial t} = \gamma\, \mu_0 \vec{M} \times \vec{H} - \frac{\alpha}{M_s} \vec{M} \times \frac{\partial \vec{M}}{\partial t} \tag{2}$$

where H is the effective magnetic field, $\gamma = 1.76 \times 10^{11} \frac{rad}{s.T}$ is the electron gyromagnetic ratio, $\mu_0 = 4\pi \times 10^{-7}$ H/m is the free space magnetic permeability, and M_s is the medium saturated static magnetization (generally assumed 0.35 T for ferrites). The LLG equation describes that the temporal variation of magnetization can be given as function of two terms: the first one (left) responsible for M precession around H and the second (right) for the motion damping due to the ferrite losses. The effective field H is a sum of two components: the azimuthal component H_θ generated by the current pulse I and the axial z-component ($H_z = H_0$) associated with the external bias, which is related to the well-known Larmor frequency ($\omega_0 = \mu_o \gamma H_0$), supposing, in this case, a medium without any interaction with another field. The azimuthal field can be calculated as a function of the current pulse amplitude I such as $H_\theta = I/\pi(b-a)$, where b and a are the outer and inner radii of the coaxial line, respectively.

Considering that the azimuthal magnetic field produced by the high-voltage pulse applied does not change the magnitude of the magnetization but only its direction because of rotational motion around H (i.e., $|\vec{M}| = M_s$ for a saturated ferrite) and that the magnetization variation in the transverse direction z is zero (i.e., $dM/dt = dM_\theta/dt$). Romanchenko *et al.* [5] developed a simplified theory to calculate the center frequency of oscillations superimposed on the amplitude of the pulse voltage propagating along the line. On these suppositions, using LLG without the dissipative term and the telegraphist equation coupled to the magnetic varying flux law given ahead by (7), they obtained the following expression for the center frequency of oscillations as:

$$f_c = \frac{\gamma}{4\pi} \mu_0 H_\theta \sqrt{1 + \frac{\chi M_s}{\mu_0 \sqrt{H_\theta^2 + H_Z^2}}} \tag{3}$$

where χ is the ferrite filling factor of the NLTL. Neglecting the first term in the square root as the second one is generally much bigger and for $H_z \gg H_\theta$ obtains

$$f_c \approx \frac{\gamma}{4\pi} \mu_0 H_\theta \sqrt{\frac{\chi M_s}{\mu_0 H_z}}. \tag{4}$$

The above-mentioned expression shows that the gyromagnetic NLTL frequency strongly depends on the amplitude of the incident pulse and on the static magnetic bias. As the pulse propagates, the azimuthal field interacts with the magnetic moments of the ferrite causing them to process at high frequency. As it can be confirmed in several papers [5], [23], the NLTL performance trend indicates that the center frequency decreases with the static magnetic field and increases with the azimuthal magnetic field produced by the input pulse amplitude. The explanation for this phenomenon is that the TEM mode wave that propagates down the coaxial line couples only to the azimuthal component of the vector

This article has been accepted for inclusion in a future issue of this journal. Content is final as presented, with the exception of pagination.

magnetization [23]. If the static magnetic bias increases, the azimuthal magnetization M decreases, lowering the frequency of oscillations. On the contrary, if the incident pulse amplitude increases, the azimuthal M contribution increases raising the frequency.

Based on the conventional theory of transmission lines [24] and on the ferrite flow relation with the current, the voltage for each segment of the transmission line is given by the magnetic flux variation per unit length, which is increased substantially by the effect of the nonlinear azimuthal magnetization M_θ of the ferrite as

$$v = \frac{d\emptyset}{dt} = L_0 \frac{dI}{dt} + \mu_0 \frac{d}{dt}\left[\int_a^b M_\theta(r)dr\right] \tag{5}$$

where L_0 is the line linear inductance per unit length in henry per meter, which for a coaxial line is

$$L_0 = \frac{\mu_0}{2\pi}\ln\left(\frac{b}{a}\right). \tag{6}$$

If the difference between a and b is not large, it can be assumed that the magnetization is uniform over the cross section of the ferrite, and thus (5) becomes

$$v = \frac{d\Phi}{dt} = L_0 \frac{dI}{dT} + \mu_0(b-a)\frac{dM_\theta}{dt}. \tag{7}$$

The corresponding unbiased line characteristic impedance is given by $Z_0 = (L_0/C_0)^{1/2}$, where C_0 is the line linear capacitance per unit length as

$$C_0 = \frac{2\pi\varepsilon_0}{\ln\left(\frac{b}{a}\right)} \tag{8}$$

where $\varepsilon_0 = 8.85 \times 10^{-12}$ F/m is the free-space permittivity. Equations (7) and (8) given earlier are very useful equations for the design of gyromagnetic lines.

II. Line Design and Experimental Setup

An experimental gyromagnetic line has been designed and tested. The coaxial gyromagnetic line is built by inserting ferrite beads through an internal conductor, where a tape sleeve is used to insulate the ferrite outer surface from the braiding. The first step for the line design is to calculate the saturated inductance in henry per meter given approximately by (6). Also, assuming $\varepsilon_R = 1$ for the ferrite, the linear capacitance in picofarad per meter was calculated by (8). For the line construction, we used Amidon ferrite beads FB43201 of 3.8 mm length and with inner and outer diameters of 1.09 and 1.93 mm, respectively. To extend up to 20 cm across the length of the internal copper wire, 53 ferrite beads were placed side by side [see Fig. 3(a)] and their outer surface was isolated from the braiding by two layers of insulating tape, forming a plastic sleeve [Fig. 3(b)]. The braiding was built using a layer of flat metallic solder wire (CT-BRAND) made of copper of 2.5 mm width [Fig. 3(c)]. This setting was kept firmly in place by welding a thin layer of tin on the copper braiding [Fig. 3(d)].

Fig. 3 (bottom) illustrates the schematics of construction steps of the coaxial line layers assembled into the external solenoid. The total linear capacitance and inductance of the line built were 22.0 pF and 18.0 μH, respectively, using an

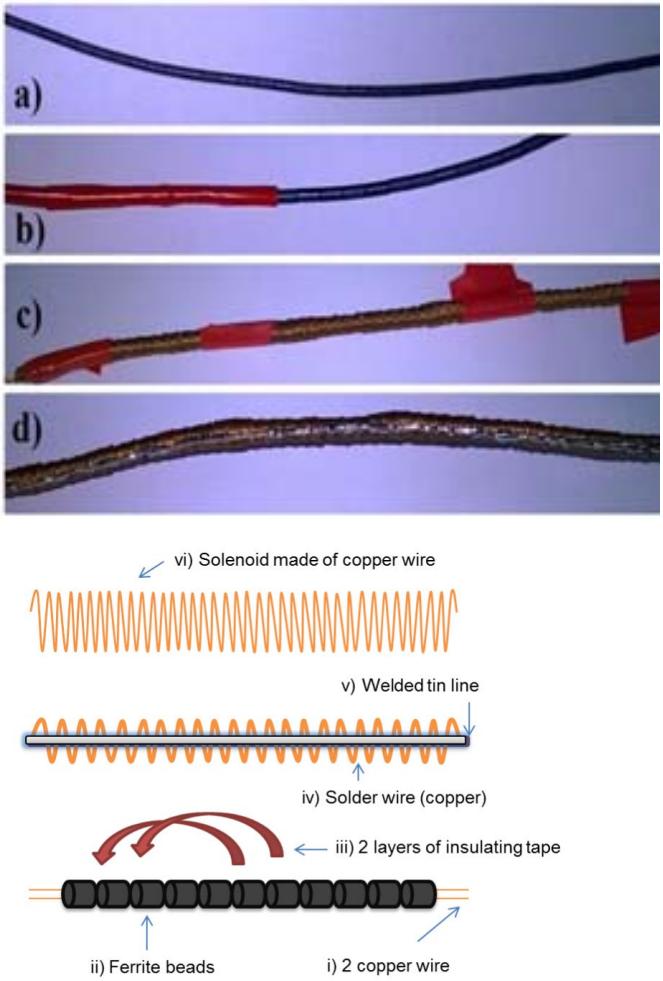

Fig. 3. Construction steps of the coaxial line are shown (top). (a) Copper wire inside the ferrite beads. (b) Insulating tape layer. (c) Solder wire layer. (d) Welded tin line. The schematics of the construction steps assembled into the solenoid are shown (bottom).

LC meter, giving an unbiased line characteristic impedance calculated of about 900 Ω.

The first setup of the experimental gyromagnetic line was completed by placing small pieces of permanent magnets over the extension of the coaxial line to produce the magnetic bias axial field. However, it was verified experimentally that the use of permanent magnets was not enough to cause the magnetic precession because of the low axial H-field produced, and therefore two different setups were built for low- and high-voltage operations. As an illustration, Fig. 4 shows the assembly used for the low-voltage operation.

Fig. 5(a) and (b) shows both the schemes employed to test the gyromagnetic line for low- and high-voltage operations, respectively, showing the pulse generator, diodes, and load (only for HV operation). In the scheme of Fig. 5(b), a stronger axial H-field is generated by an external solenoid (with 220 turns) fed by a dc current source, which encloses the coaxial line axially.

For better performance of the line, we have also used an extra bias (azimuthal) provided by another dc current source to produce the axial current through the line inner conductor, being responsible for the formation of the azimuthal field.

This article has been accepted for inclusion in a future issue of this journal. Content is final as presented, with the exception of pagination.

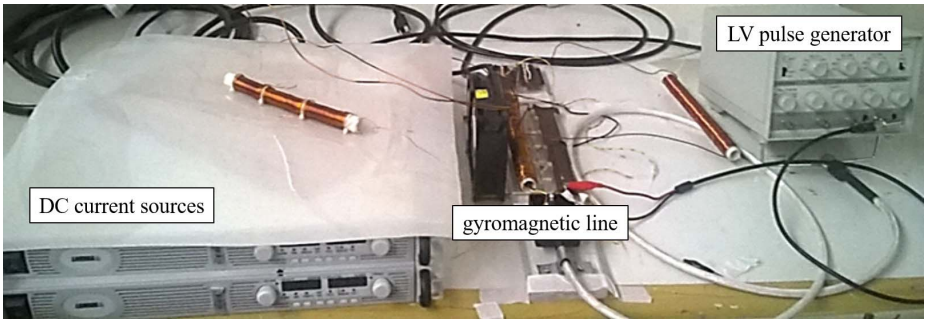

Fig. 4. Experimental assembly with axial and azimuthal bias for low-voltage operation.

To isolate the high-frequency input pulse injected onto the line from this second dc source, two extra solenoid windings (100 turns each) of high inductance are placed at input and output of the line and connected to the terminals of the dc source as shown in Fig. 5(a) and (b).

Both the signals at input and output were observed and extracted through a 4-kV/250-MHz Agilent probe linked to a 1.0-GHz digital scope from Agilent Technologies (model DSO9104A). For tests at low-voltage operation, the model TGP-110 generator was used with 10 V of pulse peak. On the other hand, at high-voltage operation the line was fed by the high-voltage pulse generator model FPG 5-1 NM, from FID Technology Company, capable of producing triangular pulses with amplitude varying in the range of 1.5–4 kV and with 2.5 ns of rise and fall times. As testing load, carbon resistors were used due to their small stray inductance and since they have solid bulk instead of spiral for conducting the current as in the case of metallic resistors of higher inductance. Five power carbon resistors of 10.0 Ω/3.0 W were connected in series to provide a 50-Ω load.

To protect the pulse generator output against reflections a BYW56 diode of 1.0-kV breakdown reverse voltage was used in series with the gyromagnetic line input.

Another five diodes of the same model connected in series at the line input were used as free-wheeling diodes for generator protection [see Fig. 5(a) and (b)].

III. Experimental Results

In this section, experimental analyzes of the gyromagnetic line performed at low- and high-voltage operations to study the magnetic precession with two magnetic biases applied simultaneously are given.

A. Low-Voltage Operation

The experimental results for the setup line configuration for low-voltage operation, proposed in Fig. 5(a), are shown in Fig. 6. One important aspect about this configuration is that the tests were performed with open terminals because with the use of the load, the input pulse rise time is too long, and it is harder to observe the gyromagnetic effect on the line at the output.

The line was fed by a pulse from a low-voltage generator (TTI-model TGP-110) with 10 V of input amplitude and 300 ns width using axial and azimuthal biases fixed at 7960 and 148 A/m, respectively.

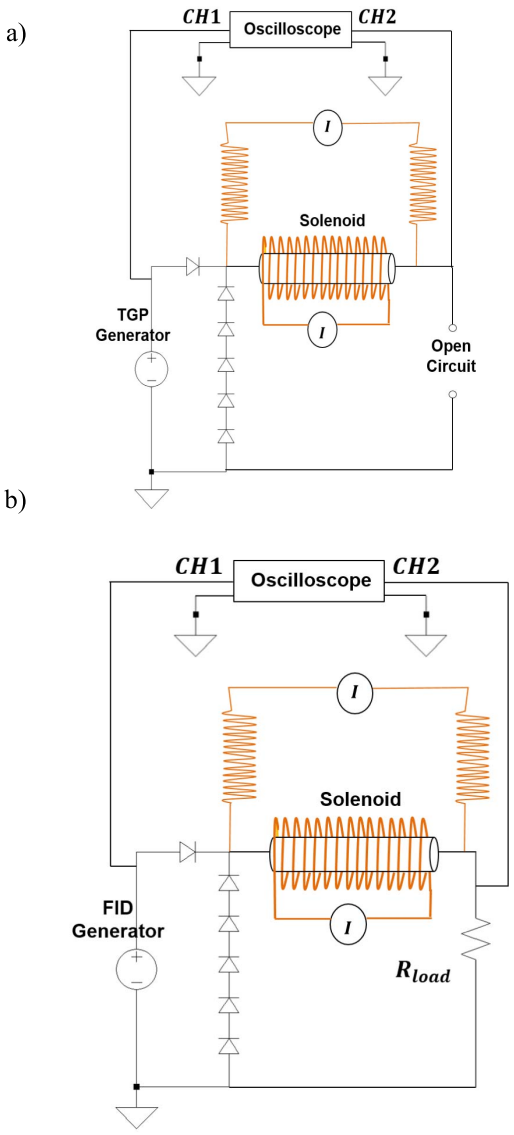

Fig. 5. Test setup of gyromagnetic line. (a) Low-voltage operation. (b) High-voltage operation.

The corresponding values of the current set at the dc sources and the magnetic field intensities in ampere per meter with the respective formulation are given in Table I. Fig. 6(a) shows the applied input pulse with a rise time of less than 100 ns. On the output pulse in Fig. 6(b), it is possible to observe the rise time of less than 50 ns with a series of oscillations

This article has been accepted for inclusion in a future issue of this journal. Content is final as presented, with the exception of pagination.

TABLE I
AXIAL AND AZIMUTHAL BIASES VALUES AT LOW-VOLTAGE TESTS

Formulation	Current (I)	Magnetic field (H)
$H_Z = NI/79.6l$ with $N = 220$ and $l = 0.2m$	8.0 A	7960 A/m
$H_\theta = I/79.6\pi d_{mean}$ with $d_{mean} = 1.51$ mm	0.7 A	148 A/m

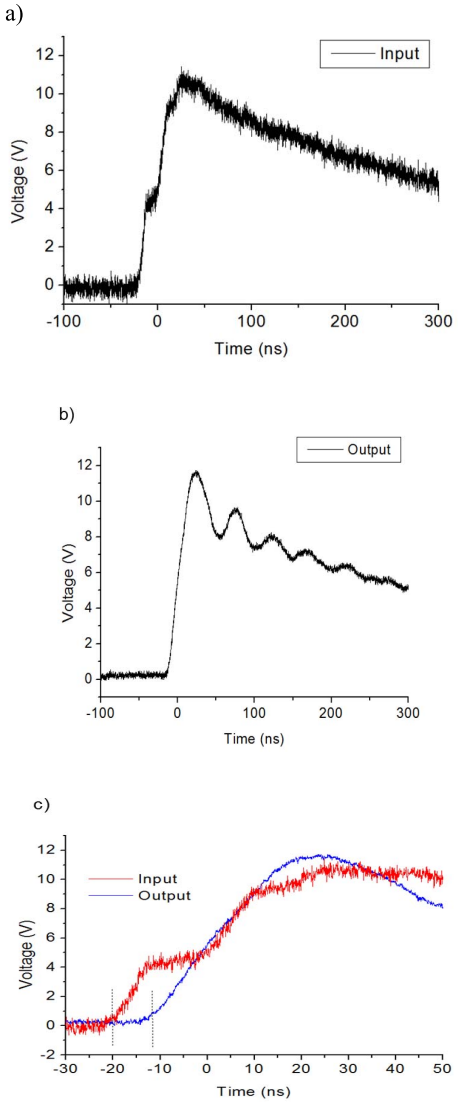

Fig. 6. Experimental results of the line with axial and azimuthal biases at low-voltage operation (a) input pulse, (b) output pulse, and (c) both pulses on shorter scale.

of considerable voltage modulation caused by the magnetic precession effect. The input and output pulses overlaid on a short scale in Fig. 6(c) show the small line delay of about 7 ns, which gives a decreased line inductance of about 3 μH at a fixed total line capacitance of the order 22 pF. The line inductance decrease observed is mainly due to the higher value of the axial magnetic bias that lowers the ferrite magnetic permeability.

Fig. 7 displays the fast Fourier transform (FFT) spectrum of the output signal where the frequency of the oscillations

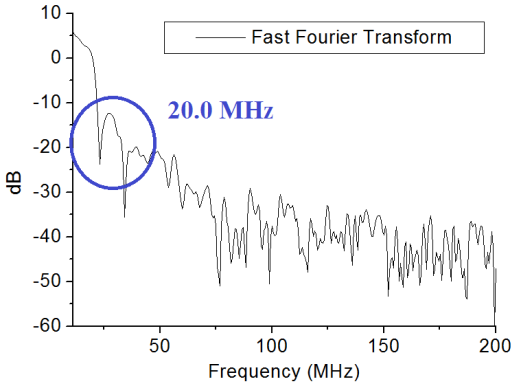

Fig. 7. Output FFT spectrum of the NLTL at low-voltage operation.

in Fig. 6(b) can be obtained at a point near the first knee on the FFT curve, 20.0 MHz approximately.

The order of magnitude of this frequency can also be obtained using (4) as $H_\theta \ll H_z$, which relates oscillation frequency with magnetic axial and azimuthal fields, where the ferrite magnetization at saturation $M_s = 0.35$ T and ferrite filling factor $\chi \approx 0.7$, considering the ferrite outer and inner diameters of 1.93 and 1.03 mm, respectively. Thus, for $H_\theta = 148$ and $H_z = 7960$ A/m, the center frequency calculated is of the order of 12 MHz, reasonably in the range of magnitude for the valued measured on FFT spectrum of about 20 MHz.

We note that when the current pulse arrives, this pulse is itself responsible for producing the azimuthal field, so it is required that this field is formed as fast as possible to have the precession effect in the ferrite at the same time of the pulse propagation, which implies a shorter rise time, about 2–3 ns. In the case of the low-voltage tests, we used axial and azimuthal biases, simultaneously. Therefore, the torque $M \times H$ is already present before the arrival of the pulse and the input pulse rise time is not necessary anymore to be shorter than 10 ns. As soon as the pulse propagates, the oscillations are induced because of the magnetic precession, but the contribution of the current pulse to the azimuthal field is not significant because of the lower amplitude of the input voltage pulse. Thus, shorter input pulse rise times are not essential as in the previous case with only axial bias. Moreover, the line worked at low voltage without any load at the output since as a longer input rise time obtained in this case makes difficult the observation of the oscillations on the propagation pulse full amplitude.

Also, we have tested the irradiation of lumped NLTLs using receiving antennas that detect oscillating signals of very small

This article has been accepted for inclusion in a future issue of this journal. Content is final as presented, with the exception of pagination.

TABLE II
AXIAL AND AZIMUTHAL BIASES VALUES AT HIGH-VOLTAGE TESTS

Formulation	Current (I)	Magnetic field (H)
$H_Z = NI/79.6l$ with $N = 220$ and $l = 0.2m$	2.10 A	2308 A/m
$H_\theta = I/79.6\pi d_{mean}$ with $d_{mean} = 1.51$ mm	0.24 A	2149 A/m

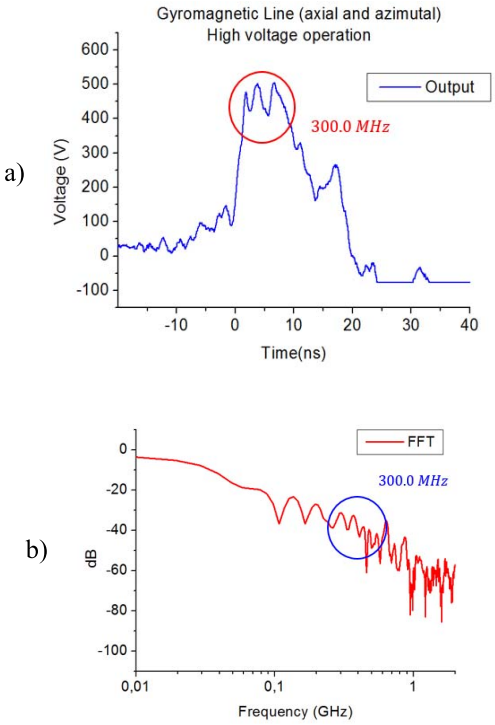

Fig. 8. Experimental results of the line with axial and azimuthal biases at high-voltage operation. (a) Line output pulse. (b) FFT spectrum.

amplitudes in the range of millivolt, which indicates that shielding to avoid external interference was not essential in our NLTL tests.

B. High-Voltage Operation

A line test was also performed at high voltage using the FID generator with axial and azimuthal bias applied simultaneously with respective dc source currents set at 2.10 and 0.24 A. The corresponding formulae for the H-field calculation are given in Table II. A current of 10.0 A through the axial line solenoid corresponds to an intensity of an external magnetic field of about 2308 A/m. However, in this case, the azimuthal field generated is given by the sum of the currents fed by the dc current source bias (0.24 A) and the high-voltage pulse applied, which is of the order of 10.24 A (10 + 0.24 A), considering the peak amplitude of the output pulse obtained of about 500 V into a load of 50 Ω. Thus, in this case, the use of azimuthal bias could be disregarded in principle as 0.24 A $\ll$ 10 A. Anyway, the total value of 10.24 A corresponds to an effective azimuthal field of the order of 2149 A/m. To obtain the result in Fig. 8(a), the FID generator of fast rise time (1.0 ns) was used to produce an input pulse with peak of about 2500 V with an approximate Gaussian shape of 5.0 ns width.

As observed in Fig. 8(a), the lower pulse peak amplitude at output is due to the negative reflection coefficient as the load resistance is 50 Ω and the stressed line impedance is higher (of the order of 450 Ω) since the ferrite is not heavily saturated under this condition.

Moreover, the output voltage is limited by the maximum voltage provided by the high-voltage FID pulse generator.

Fig. 8(b) shows the FFT spectrum of the output pulse. Although not very clear in the FFT spectrum, the oscillation frequency appears to be in the range of 300–400 MHz. In fact, this value can be confirmed using (3) as H_θ and H_z are of the same order, where χ is assumed to be 0.7 and $M_s = 0.35$ T. For $H_z = 2308$ A/m and $H_\theta = 2149$ A/m, (3) gives a center frequency near 300 MHz, which is of the order of magnitude seen in the FFT in Fig. 8(b). It is important to highlight that it was not achieved a better signal at the output of the gyromagnetic line due to the voltage limitation of the high-voltage FID pulser (4 kV) and due to the load impedance mismatch as ferrite was not heavily saturated.

IV. CONCLUSION

According to the results obtained from the experimental analysis, it was observed that when the axial bias is increased, the frequency and output pulse rise time decrease. Moreover, it was noted that the azimuthal bias has direct relation with the modulation of the output pulse and a slight influence on the output rise time compression. At low-voltage operation with open circuit at the end of the line, good modulation of the output pulse was obtained, although the slow rise time of the input pulse makes it difficult to observe the gyromagnetic effect. At high-voltage operation, the frequency generated by the gyromagnetic line was around 300-MHz. NLTL frequency has a stronger dependence on the amplitude of the input pulse at high voltage as azimuthal field is generated by the resulting pulse current. Application of simultaneous biases (axial and azimuthal) was essential for RF generation in tens of megahertz at low-voltage operation with open circuit at the line output side as azimuthal field is generated only by the dc bias current through the line. However, for high-voltage operation the application of both biases is important only in the case with reduced pulse current since the radial field produced by the line dc bias current will be added to the pulsed azimuthal field. In this situation, depending on the value of the dc current bias required to compensate the operation with lower pulse current a system cooling will be needed to avoid overheating of the line material.

This article has been accepted for inclusion in a future issue of this journal. Content is final as presented, with the exception of pagination.

The development of gyromagnetic lines demands additional research on new nonlinear magnetic materials of high magnetization at saturation for lower pulse current (low-voltage operation) and with good performance in the harsh conditions of space.

REFERENCES

[1] W. J. Larson and J. R. Wertz, *Space Mission Analysis and Design*, 3rd ed. Norwell, MA, USA: Kluwer, 2005.

[2] R. D. Briskman and M. A. R. Kaliski, "Transmitter microdischarges in communications and broadcast satellites," *Acta Astronautica*, vol. 126, pp. 163–167, Sep./Oct. 2016.

[3] A. Moreira. (Jul. 2013). *Synthetic Aperture Radar (SAR): Principles and Applications*. [Online]. Available: https://earth.esa.int/documents/10174/642943/6-LTC2013-SAR-Moreira.pdf

[4] A. Passaro, M. M. da Silva Costa, and, O. L. Bogossian, "Basic Requirements for synthetic aperture radar satellite mission," in *Proc. Conf. 6th Workshop Space Eng. Technol.*, 2015, pp. 1–3. [Online]. Available: http://urlib.net/8JMKD3MGP3W34P/3L8HBTL

[5] I. V. Romanchenko, V. V. Rostov, A. V. Gunin, and V. Y. Konev, "High power microwave beam steering based on gyromagnetic nonlinear transmission lines," *J. Appl. Phys.*, vol. 117, no. 21, p. 214907, 2015.

[6] V. V. Rostov *et al.*, "Generation of sub-GW RF pulses in nonlinear transmission lines," in *Proc. IEEE Int. Pulse Power Conf. (PPC)*, Washington, DC, USA, Jun./Jul. 2009, pp. 70–73.

[7] I. V. Romanchenko, V. V. Rostov, V. P. Gubanov, A. S. Stepchenko, A. V. Gunin, and I. K. Kurkan, "Repetitive sub-gigawatt RF source based on gyromagnetic nonlinear transmission line," *Rev. Sci. Instrum.*, vol. 83, no. 7, p. 074705, 2012.

[8] D. V. Reale, J. M. Parson, A. A. Neuber, J. C. Dickens, and J. J. Mankowski, "Investigation of a stripline transmission line structure for gyromagnetic nonlinear transmission line high power microwave sources," *Rev. Sci. Instrum.*, vol. 87, no. 3, p. 034706, 2016.

[9] D. V. Reale *et al.*, "Bias-field controlled phasing and power combination of gyromagnetic nonlinear transmission lines," *Rev. Sci. Instrum.*, vol. 85, no. 5, p. 054706, 2014.

[10] N. Seddon, C. R. Spikings, and J. E. Dolan, "RF pulse formation in nonlinear transmission lines," in *Proc. 16th IEEE Int. Pulsed Power Conf.*, Albuquerque, NM, USA, Jun. 2007, pp. 678–681.

[11] M. P. Brown and P. W. Smith, "High power, pulsed soliton generation at radio and microwave frequencies," in *IEEE Int. Pulsed Power Conf. Dig. Tech. Papers*, Baltimore, MD, USA, Jun./Jul. 1997, pp. 346–354.

[12] P. W. Smith, *Transient Electronics: Pulsed Circuit Technology*. Hoboken, NJ, USA: Wiley, 2002, pp. 237–264.

[13] C. R. Spikings, N. Seddon, R. A. Ibbotson, and J. E. Dolan, "HPM systems based on NLTL technologies," in *Proc. IET Conf. High Power RF Technol.*, London, U.K., Feb. 2009, pp. 1–3.

[14] J. O. Rossi, L. P. S. Neto, F. S. Yamasaki, and J. J. Barroso, "State of the art of nonlinear transmission lines for applications in high power microwaves," in *Proc. SBMO/IEEE MTT-S Int. Microw. Optoelectr. Conf. (IMOC)*, Rio de Janeiro, Brazil, Aug. 2013, pp. 1–5.

[15] F. S. Yamasaki, L. P. S. Neto, J. O. Rossi, and J. J. Barroso, "Soliton generation using nonlinear transmission lines," *IEEE Trans. Plasma Sci.*, vol. 42, no. 11, pp. 3471–3477, Nov. 2014.

[16] J. Gaudet, E. Schamiloglu, J. O. Rossi, C. J. Buchenauer, and C. Frost, "Nonlinear transmission lines for high power microwave applications—A survey," in *Proc. IEEE Int. Power Modulators High Voltage Conf. (IPMHVC)*, Las Vegas, NV, USA, May 2008, pp. 131–138.

[17] J. O. Rossi and P. N. Rizzo, "Study of hybrid nonlinear transmission lines for high power RF generation," in *Proc. IEEE Int. Pulsed Power Conf. (PPC)*, Washington, DC, USA, Jun./Jul. 2009, pp. 46–50.

[18] F. S. Yamasaki, E. Schamiloglu, J. O. Rossi, and J. J. Barroso, "Spice simulations of nonlinear gyromagnetic lines," in *Proc. IEEE Int. Pulsed Power Conf. (PPC)*, Austin, TX, USA, May/Jun. 2015, pp. 1–6.

[19] F. S. Yamasaki, E. Schamiloglu, J. O. Rossi, and J. J. Barroso, "Simulation studies of distributed nonlinear gyromagnetic lines based on LC lumped mode," *IEEE Trans. Plasma Sci.*, vol. 44, no. 10, pp. 2232–2239, Oct. 2016.

[20] F. S. Yamasaki, J. O. Rossi, J. J. Barroso, and E. Schamiloglu, "Analysis of a gyromagnetic nonlinear transmission line based on experimental results," in *Proc. Euro-Asian Pulsed Power Conf. (EAPPC)*, Estoril, Portugal, Sep. 2016, p. 155.

[21] F. S. Yamasaki, "Simulation and experimental characterization of gyromagnetic nonlinear transmission lines for prospective aerospace applications," Ph.D. dissertation, Plasma Lab. Dept., Plasma Lab., INPE, São José dos Campos, Brazil, 2017.

[22] T. L. Gilbert, "A phenomenological theory of damping in ferromagnetic materials," *IEEE Trans. Magn.*, vol. 40, no. 6, pp. 3443–3449, Nov. 2004.

[23] J. W. B. Bragg, J. C. Dickens, and A. A. Neuber, "Material selection considerations for coaxial, ferrimagnetic-based nonlinear transmission lines," *J. Appl. Phys.*, vol. 113, no. 6, p. 064904, 2013.

[24] J. E. Dolan, "Simulation of shock waves in ferrite-loaded coaxial transmission lines with axial bias," *J. Phys. D: Appl. Phys.*, vol. 32, no. 15, pp. 1826–1831, 1999.

Fernanda S. Yamasaki (M'15) was born in Cruzeiro, Brazil, in 1988. She received the B.Sc. degree in telecommunication technology from the University of Campinas, Campinas, Brazil, in 2010, and the M.Sc. and D.Sc. degrees in engineering and space technology from the National Institute for Space Research (INPE), Sao Jose dos Campos, Brazil, in 2013 and 2017, respectively.

Since 2010, she has been with INPE, where she is involved in nonlinear transmission lines for RF generation. From 2011 to 2013, she developed spice models to simulate nonlinear dielectric lines. Her current research interests include the study of RF generation using nonlinear gyromagnetic lines for applications in space technologies.

Dr. Yamasaki was a recipient of the Best Student Paper Award on gyromagnetic line simulations at the 2015 IEEE International Pulsed Power Conference.

Jose O. Rossi (M'05–SM'12) received the B.Sc. degree in electrical engineering from Campinas University, Campinas, Brazil, in 1982, the M.Sc. degree in electronics from the Technological Institute of Aeronautics, São Jose dos Campos, Brazil, in 1992, and the D.Phil. degree in engineering science from Oxford University, Oxford, U.K., in 1998, with a focus on pulsed power systems and transmission line transformers

Since 1983, he has been with the Associated Plasma Laboratory, National Institute for Space Research (INPE), Sao Jose dos Campos, Brazil, where he is involved in pulsed power generators for microwave generation and surface treatment by plasma implantation. From 2007 to 2008, he was a Visiting Scientist with the Department of Electrical and Computer Engineering, University of New Mexico, Albuquerque, NM, USA, where he was involved in dielectrics of high breakdown strength for compact energy storage systems. Since 2015, he has been the Head of the Associated Plasma Laboratory with INPE. His current research interests include plasma surface processing applications, nonlinear transmission lines, and high-voltage ceramic dielectrics used in the development of compact pulsed power supplies and RF generation sources for space, defense systems.

Dr. Rossi is a member of Brazilian Power Electronics and Physical Societies as well as a Consultant on research projects for the State of Sao Paulo Research Foundation, FAPESP, Brazil.

This article has been accepted for inclusion in a future issue of this journal. Content is final as presented, with the exception of pagination.

Joaquim J. Barroso (M'08) received the B.S. degree in electronics engineering and the M.S. degree in plasma physics from the Technological Institute of Aeronautics (ITA), São José dos Campos, Brazil, in 1976 and 1980, respectively, and the Ph.D. degree in plasma physics from the National Institute for Space Research (INPE), São José dos Campos, in 1988.

He was with INPE, where he was involved in the design and construction of high-power microwave tubes. From 1989 to 1990, he was a Visiting Scientist with the Massachusetts Institute of Technology, Cambridge, MA, USA. He is currently a Senior Visiting Professor with ITA supported by the Brazilian Funding Agency CAPES. His current research interests include microwave electronics, plasma technology, electromagnetics, and metamaterials.

Edl Schamiloglu (M'90–SM'95–F'02) received the B.S. degree in applied physics and nuclear engineering and the M.S. degree in plasma physics from Columbia University, New York, NY, USA, in 1979 and 1981, respectively, and the Ph.D. degree in engineering (minor in mathematics) from Cornell University, Ithaca, NY, USA, in 1988.

In 1988, he joined the University of New Mexico (UNM), Albuquerque, NM, USA, as an Assistant Professor, where he is currently a Distinguished Professor with the Department of Electrical and Computer Engineering and directs the Pulsed Power, Beams, and Microwaves Laboratory. He co-edited Advances in *High Power Microwave Sources and Technologies* (Piscataway, NJ, USA: IEEE, 2001) (with R. J. Barker) and co-authored *High-Power Microwaves* (Boca Raton, FL, USA: CRC Press, 3rd edition, 2015) (with J. Benford and J. Swegle), over 125 refereed journal papers, over 200 reviewed conference papers. He holds six patents.

Dr. Schamiloglu was a recipient of the 2013 IEEE Nuclear and Plasma Sciences Society's Richard F. Shea Distinguished Member Award, the 2014 International Electrotechnical Commission 1906 Award Recognizing an Expert's Exceptional Current Achievements, and the 2015 IEEE NPSS Peter Haas Award, which recognizes outstanding contributions to pulsed power technology resulting from an individual's continued effort to develop programs of research education, and information exchange that are the basis for progress in pulsed power.